Journal of Microelectronics and Electronic Packaging (2010) **7**, 90-98

ISSN: 1551-4897

Effects of Nonuniform Base Heating on Single Stack and Multi-Stack Microchannel Heat Sinks Used for Electronics Cooling

Pradeep Hegde[1,*] and K.N. Seetharamu[2]

Abstract—**Numerical investigations with regard to the thermal characteristics of water cooled single stack and multistack microchannel heat sinks subjected to nonuniform base heating are conducted. Nonuniformities in base heating are accomplished by applying gradually increasing and gradually decreasing base heat fluxes with respect to coolant flow direction in the heat sink. The effects of heat concentration upstream, downstream, and in the center half of the microchannel heat sinks (similar to a hotspot) are also studied. Both parallel flow and counter coolant flow conditions in the heat sink are considered and the results are compared. The results are presented in the form of base temperature distribution and heat sink thermal resistance. The finite element method is used for the analysis.**

Keywords—**Microchannel, stacked heat sink, thermal resistance, nonuniform base heating, finite element method**

Introduction

Liquid cooled microchannel heat sinks are one of the most effective heat removal techniques from the high heat flux and space constrained electronic devices. Tuckerman and Pease [1] were the first to show that electronic chips could be effectively cooled by forced fluid flow through microchannels etched directly on the back of the silicon wafer. Phillips [2] developed a thermal resistance model to estimate the thermal resistance of microchannel heat sinks. Kim and Kim [3] analyzed laminar heat transfer in microchannel heat sinks by using the modified Darcy model for fluid flow and the two-equation model for heat transfer. Fedorov and Viskanta [4] developed a three-dimensional model to investigate the conjugate heat transfer in a microchannel heat sink for electronic packaging applications. Kulkarni and Das [5] developed analytical and numerical methods to analyze single layer microchannel heat sinks, considering the effects of radiation heat transfer. Hegde [6] and Hegde et al. [7, 8] have investigated both single phase and two phase flows in single stack and multistack microchannel heat sinks using the finite element method. Naphon and Khonseur [9] experimentally investigated the heat transfer characteristics and pressure drop in air cooled microchannel heat sinks.

Further reduction in thermal resistance and the wall temperatures can be achieved by using multistack microchannel heat sinks. Chong et al. [10] modeled single layer counter flow and double layer counter flow microchannel heat sinks using a thermal resistance network. Wei and Joshi [11] analyzed stacked silicon microchannel heat sinks with a parallel flow arrangement.

A further challenging aspect is the nonuniform heat flux distribution in electronic chips and devices. In a high power application such as a server chip, the nonuniform heat distribution may lead to peak heat fluxes which are far greater than the average heat flux over the entire chip surface. Large fluctuations of temperature as well as large spatial variations of temperature in the equipment become responsible for thermal stresses, malfunctions, and eventual breakdown of the equipment. The purpose of thermal design is to create and maintain throughout the equipment a temperature distribution having limited variations around a moderate level. It can be observed from the literature that only few investigators [7, 11] have looked into the effects of nonuniform base heating in microchannel heat sinks.

In the present work, the effects of nonuniform base heating on the performance of water cooled single stack and stacked microchannel heat sinks of rectangular cross section are analyzed. The results are compared with those for uniform base heating. The finite element method is used for the analysis wherein a self developed 12 noded element is used for channel discretization. Heat sink channels with a hydraulic diameter of less than 130 μm are used for analysis.

Methodology

Microchannel heat sinks with rectangular cross section channels are analyzed. Taking advantage of symmetry, a single pair of adjacent channels of the heat sink is considered for analysis. A 12 node finite element representing a pair of adjacent microchannels is used for the finite element modeling. A typical element used for the discretization of a parallel flow heat sink is shown in Fig. 1. Nodes 5 and 6 of the

Manuscript received February 2010 and accepted August 2010
[1]Engineering Department, Mechanical Engineering, Salalah College of Technology, Oman
[2]Department of Mechanical Engineering, P.E.S. Institute of Technology, Bangalore, India
*Corresponding author; email: pghegde@gmail.com

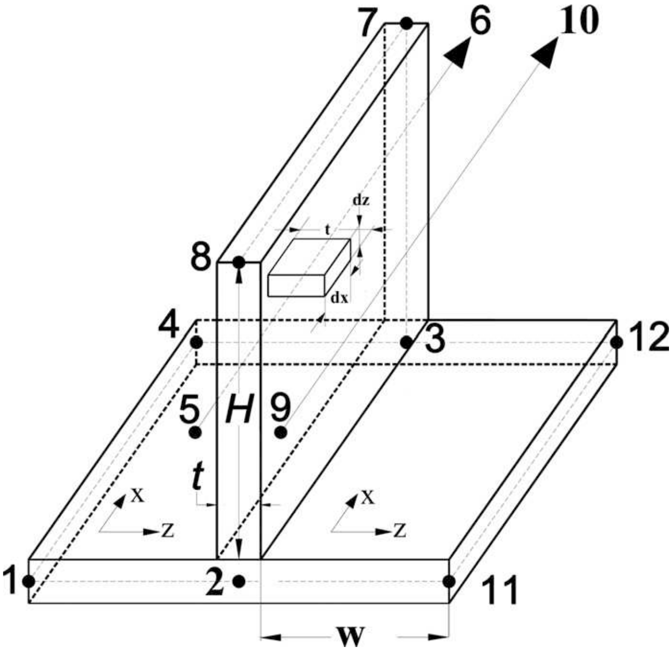

Fig. 1. The 12 node finite element used for the discretization of parallel flow microchannel heat sinks.

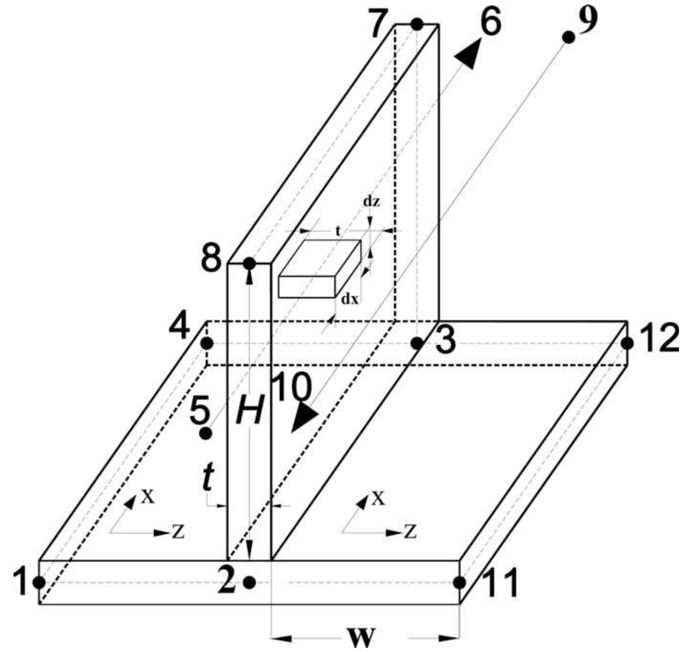

Fig. 2. The 12 node finite elements used for the discretization of counterflow microchannel heat sinks.

element represent the coolant flow in the left channel while nodes 9 and 10 represent the coolant flow in the adjacent right channel. Nodes 2-3-7-8 represent the dividing wall between the two channels, and nodes 1-2-3-4 and 2-11-12-3 represent the left and right bottom walls, respectively. The element as a whole is actually an assembly of four noded bilinear rectangular elements and two noded linear elements. The microchannel bottom and dividing walls are constituted by the bilinear rectangular elements, while the coolants are discretized by two noded linear elements, the two fluid nodes being located at the inlet and the outlet of the overall cell. The base of the microchannel receives heat from the source and the heat is transferred to the coolant by convection from the base and the dividing wall. The entire element is repeatable in the sense that a suitable number of elements can be assembled in the lengthwise and lateral directions to constitute a complete microchannel heat sink. A similar element with opposite coolant flow directions in adjacent channels (Fig. 2) is used for the discretization of single layer counterflow heat sinks. A typical assembly of elements in the streamwise direction for single stack parallel flow and single stack counterflow heat sinks are shown in Figs. 3 and 4. The element assembly for a double stack parallel flow heat sink is shown in Fig. 5 and for a double stack counterflow heat sink is shown in Fig. 6.

The governing equations of heat transfer are obtained by performing an energy balance on a control volume in the walls and the coolant of the individual elements, which make the pair of channels. Assumptions of steady state flow and heat transfer, negligible radiation heat transfer, and averaged convective heat transfer coefficient h for the cross section are made for the analysis.

In order to obtain the governing equations for the walls, conduction in two directions is considered, that is, in the streamwise direction and along the height of the microchannel for the dividing wall or the width of the channel for bottom wall. The base heat flux is the thermal input to the channel, while the heat lost to the coolant is the output.

Nomenclature

Ar = Aspect ratio
B = Width of the heat sink, m
C_p = Specific heat of coolant at constant pressure J/kg K
G = Coolant mass flux, kg/m^{2}s
H = Microchannel depth, m
W = Width of the microchannel
h = Heat transfer coefficient, W/m^2 K
I = Coolant enthalpy, J/kg
k = Thermal conductivity, W/m K
L = Length of the microchannel, m
L_e = Length of a single element, m
$\dot{m}$ = Mass flow rate of the coolant, kg/s
q = Base heat flux, W/cm^2
R = Thermal resistance, °C/W
T_f = Coolant temperature, °C
$T_{f,i}$ = Coolant inlet temperature, °C
T_{sat} = Coolant saturation temperature, °C
t = Microchannel fin thickness, m
w = half width of the microchannel, m

Subscripts

counter = Counter flow arrangement
parallel = Parallel flow arrangement
sp = Single-phase flow
tp = Two-phase flow
L = Left channel
R = Right channel

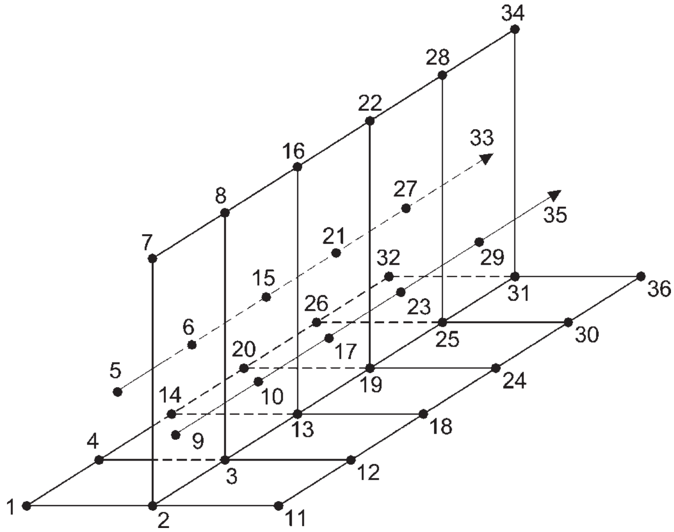

Fig. 3. Typical assembly of elements in the streamwise direction for a single stack parallel flow heat sink.

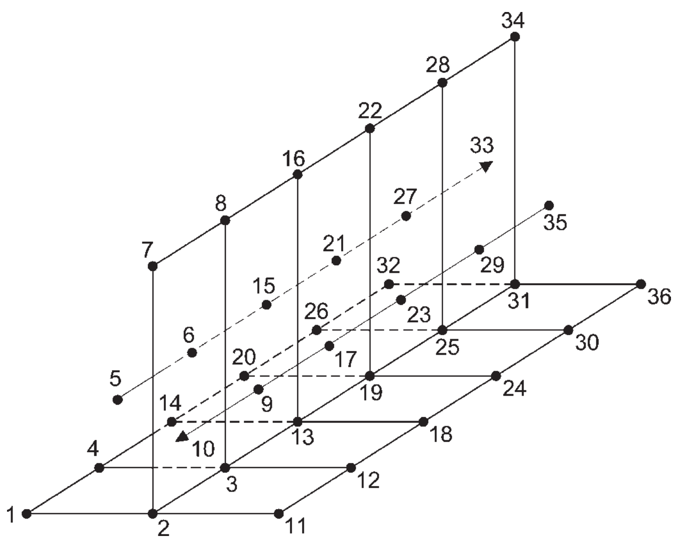

Fig. 4. Typical assembly of elements in the streamwise direction for a single stack counterflow heat sink.

The two-dimensional energy balance equation for the central wall of the element (2-3-7-8) can be written as:

$$k\frac{\partial^2 T_{\mathrm{cw}}}{\partial x^2}+k\frac{\partial^2 T_{\mathrm{cw}}}{\partial z^2}-\frac{h}{t}(T_{\mathrm{cw}}-T_{\mathrm{f,L}})-\frac{h}{t}(T_{\mathrm{cw}}-T_{\mathrm{f,R}})=0 \quad (1)$$

Similarly, for the bottom wall of the left channel (1-2-3-4), the energy balance equation is:

$$k\frac{\partial^2 T_{\mathrm{b,L}}}{\partial x^2}+k\frac{\partial^2 T_{\mathrm{b,L}}}{\partial y^2}-\frac{h}{t}(T_{\mathrm{b,L}}-T_{\mathrm{f,L}})=0 \quad (2)$$

for the bottom wall of the right channel (2-11-12-3):

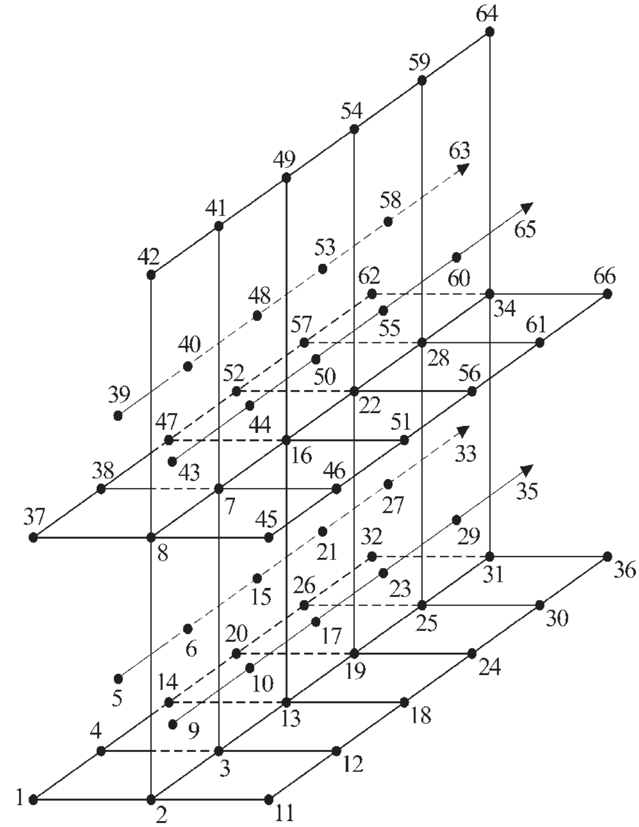

Fig. 5. Typical assembly of elements and node numbering for a double stack parallel flow microchannel heat sink.

$$k\frac{\partial^2 T_{\mathrm{b,R}}}{\partial x^2}+k\frac{\partial^2 T_{\mathrm{b,R}}}{\partial y^2}-\frac{h}{t}(T_{\mathrm{b,R}}-T_{\mathrm{f,R}})=0 \quad (3)$$

The energy balance equation for the coolant in the left channel (5-6) that receives heat from the central wall and the bottom wall of the channel can be written as:

$$\dot{m}\frac{dI_{\mathrm{L}}}{dx}=hH(T_{\mathrm{cw}}-T_{\mathrm{f,L}})+hw_{\mathrm{L}}(T_{\mathrm{b,L}}-T_{\mathrm{f,L}}) \quad (4)$$

Similarly, for the fluid in the right channel (9-10):

$$\dot{m}\frac{dI_{\mathrm{R}}}{dx}=hH(T_{\mathrm{cw}}-T_{\mathrm{f,R}})+hw_{\mathrm{R}}(T_{\mathrm{b,R}}-T_{\mathrm{f,R}}) \quad (5)$$

where T_{cw} is the temperature of the central wall of the element; $T_{\mathrm{b,L}}$ and $T_{\mathrm{b,R}}$ are the temperatures of the bottom walls of the left and right channels of the element; and $T_{\mathrm{f,L}}$ and $T_{\mathrm{f,R}}$ are fluid temperatures in the left and right channels, respectively. H is the depth of the microchannel, and w_{L} and w_{R} are the half widths of the left and right microchannels, respectively. Also, $h = h_{\mathrm{sp}}$ for single-phase flow, whereas $h = h_{\mathrm{tp}}$ and $T_{\mathrm{f}} = T_{\mathrm{sat}}$ for two-phase flow. The single phase heat transfer coefficient is obtained from [12]. The finite element formulation of the above set of equations can be conceived by considering the microchannel

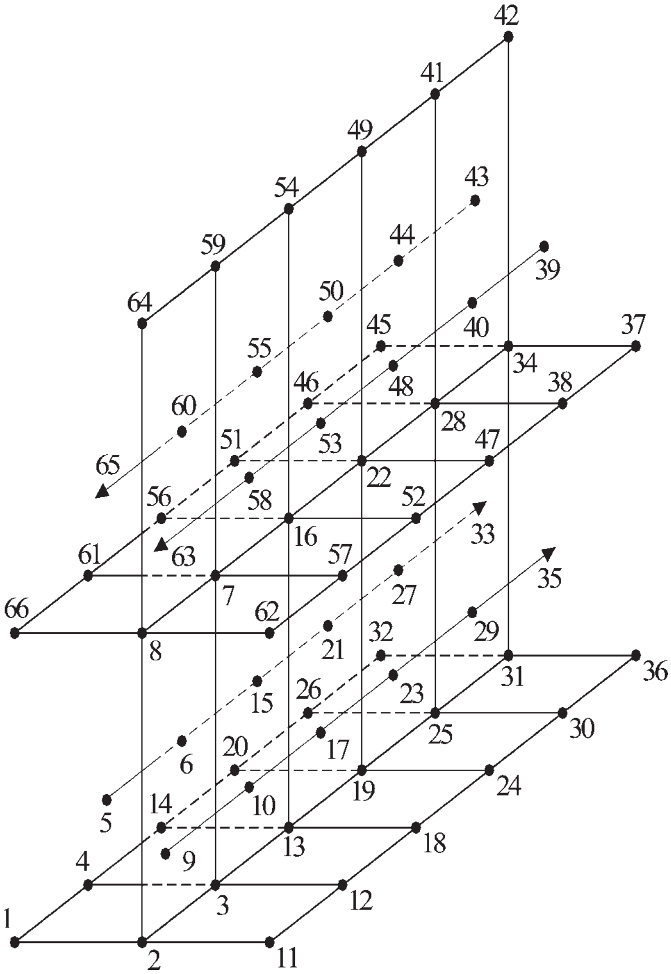

Fig. 6. Typical assembly of elements and node numbering for a double stack counterflow microchannel heat sink.

wall as bilinear rectangular element and the coolant as two node linear element. The microchannel wall temperature is assumed to vary as:

$$T = \sum_{i=1}^{i=4} N_i T_i \tag{6}$$

where the shape function N_i for a general quadrilateral element is given as [13]:

$$N_i = \frac{1}{4}(1 + \xi\xi_i)(1 + \eta\eta_i) \tag{7}$$

where, η_i, ξ_i are the local coordinates of the corner node i.

The coolant enthalpy is assumed to vary linearly as:

$$I_L = \sum_{j=5}^{j=6} N_j I_j, \; I = \sum_{j=9}^{j=10} N_j I_j \tag{8}$$

The shape functions for the linear element are given as [13]:

$$N_1 = 1 - \frac{x}{L_e}, \; N_2 = \frac{x}{L_e} \tag{9}$$

The temperature driving potential for the convective heat transfer is assumed to be the difference between average wall and fluid temperatures. Therefore,

$$(T_{cw} - T_{f,L}) = \frac{1}{4}(T_2 + T_3 + T_7 + T_8) - \frac{1}{2}(T_5 + T_6) \tag{10}$$

$$(T_{cw} - T_{f,R}) = \frac{1}{4}(T_2 + T_3 + T_7 + T_8) - \frac{1}{2}(T_9 + T_{10}) \tag{11}$$

$$(T_{b,L} - T_{f,L}) = \frac{1}{4}(T_1 + T_2 + T_3 + T_4) - \frac{1}{2}(T_5 + T_6) \tag{12}$$

$$(T_{b,R} - T_{f,R}) = \frac{1}{4}(T_2 + T_{11} + T_{12} + T_3) - \frac{1}{2}(T_9 + T_{10}) \tag{13}$$

Applying the Galerkin weighted residual integral to the governing equations, we write the complete set of equations as:

$$[K_e]\{T\} = \{f_e\} \tag{14}$$

The element matrix $[K_e]$ is of the order 12×12 and can be written as:

$$K_e = \begin{bmatrix} A_1 & B_1 & C_1 & D_1 & E_2 & E_2 & 0 & 0 & 0 & 0 & 0 & 0 \\ B_1 & 2A_1 + A_2 & 2D_1 + B_2 & C_1 & E_1 + E_2 & E_1 + E_2 & C_2 & D_2 & E_1 + E_2 & E_1 + E_2 & B_1 & C_1 \\ C_1 & 2D_1 + B_2 & 2A_1 + A_2 & B_1 & E_1 + E_2 & E_1 + E_2 & D_2 & C_2 & E_1 + E_2 & E_1 + E_2 & C_1 & B_1 \\ D_1 & C_1 & B_1 & A_1 & E_2 & E_2 & 0 & 0 & 0 & 0 & 0 & 0 \\ W & U + W & U + W & W & H_1 & I_1 & U & U & 0 & 0 & 0 & 0 \\ W & U + W & U + W & W & H_1 & I_1 & U & U & 0 & 0 & 0 & 0 \\ 0 & C_2 & D_2 & 0 & E_1 & E_1 & A_2 & B_2 & E_1 & E_1 & 0 & 0 \\ 0 & D_2 & C_2 & 0 & E_1 & E_1 & B_2 & A_2 & E_1 & E_1 & 0 & 0 \\ 0 & U + W & U + W & 0 & 0 & 0 & U & U & H_1 & I_1 & W & W \\ 0 & U + W & U + W & 0 & 0 & 0 & U & U & H_1 & I_1 & W & W \\ 0 & B_1 & C_1 & 0 & 0 & 0 & 0 & 0 & E_2 & E_2 & A_1 & D_1 \\ 0 & C_1 & B_1 & 0 & 0 & 0 & 0 & 0 & E_2 & E_2 & D_1 & A_1 \end{bmatrix} \tag{15}$$

where

$$A_1 = 2e_{x2} + 2e_y + c_b,\ B_1 = -2e_{x2} + e_y + c_b,$$

$$C_1 = -e_{x2} + e_y + c_b,\ D_1 = e_{x2} - 2e_y + c_b,$$

$$E_1 = \frac{-2c_f}{C_p},\ H_1 = \frac{-f_m - 2(U+W)}{C_p},\ I_1 = \frac{f_m - 2(U+W)}{C_p},$$

$$U = \frac{hL_eH}{8},\ W = \frac{-hL_ew}{8},$$

$$A_2 = 2e_{x1} + 2e_z + 2c_f,\ B_2 = -2e_{x1} + e_z + 2c_f,$$

$$C_2 = -e_{x1} - e_z + 2c_f,\ D_2 = e_{x1} - 2e_z + 2c_f,$$

$$E_2 = \frac{-2c_b}{C_p},\ e_{x1} = \frac{tkH}{6L_e},\ e_{x2} = \frac{tkw}{6L_e},\ e_z = \frac{tkL_e}{6H},\ e_y = \frac{tkL_e}{6w},$$

$$c_f = \frac{hL_eH}{16},\ c_b = \frac{hL_ew}{16},\ f_m = \frac{\dot{m}C_p}{2}.$$

Considering the heat flux at the base of the element, the element force vector can be written as:

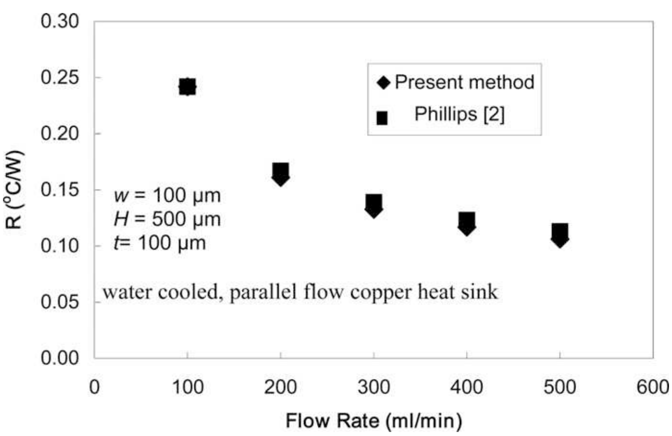

Fig. 7. Thermal resistances at different flow rates for a 10 mm × 10 mm single stack heat sink.

$$\{f_e\} = \frac{q(w+0.5t)L_e}{4}[1\ \ 2\ \ 2\ \ 1\ \ 0\ \ 0\ \ 0\ \ 0\ \ 0\ \ 0\ \ 1\ \ 1]^T \tag{16}$$

The vector of unknowns $\{T\}$ can be written as:

$$\{T\} = [T_1\ \ T_2\ \ T_3\ \ T_4\ \ I_5\ \ I_6\ \ T_7\ \ T_8\ \ I_9\ \ I_{10}\ \ T_{11}\ \ T_{12}]^T \tag{17}$$

wherein the coolant enthalpy $I = C_pT_f$. Converging results are obtained with less than 20 elements assembled in the streamwise direction (20 elements per stack for stacked heat sinks). The globalized matrix equation is solved with the boundary condition of known fluid inlet temperature using MATLAB, to determine the microchannel wall temperature distribution and the coolant enthalpies or temperature at each node in the streamwise direction. The final results of the analysis are presented in the form of thermal resistances of the microchannel heat sinks. The thermal resistance of the microchannel heat sink is obtained from the relation:

$$R = \frac{(T_{max} - T_{f,i})}{qLB} \tag{18}$$

where T_{max} is the maximum microchannel wall temperature.

Results and Discussion

Fig. 7 gives the comparison of thermal resistances at different coolant flow rates, obtained by the present method with those obtained by the thermal resistance model [2] for a liquid cooled single stack parallel flow microchannel heat sink. Note from Fig. 7 that good agreement exists between the two results.

Table I compares the thermal resistances obtained by the present method for a 10 mm × 10 mm water cooled, double stack counterflow heat sink with those obtained by [10] for different channel dimensions. It can be observed from Table I that good agreement exists between the results obtained by the two methods.

The above comparisons validate the ability of the present method to analyze the thermal performance of microchannel heat sinks with either parallel flow or counterflow of the coolant in single or multistack heat sinks.

Table I
Comparison of Thermal Resistances for Water Cooled, Double Stack, Counterflow, Silicon Microchannel Heat Sinks with Different Channel Dimensions

Microchannel dimensions (µm)	Coolant flow velocity (m/s)	R (°C/W) Present method	R (°C/W) [2] (Thermal resistance model)	R (°C/W) [2] (3D-CFD results)	% Deviation From thermal resistance model	% Deviation From 3D-CFD results
$H = 100$, $w = 100$, $t = 100$	2.5	0.223	0.236	0.221	5.5	0.9
$H = 449.25$, $w = 252.9$, $t = 113.17$	8.53	0.0656	0.066	NA	0.6	NA
$H = 365.98$, $w = 86.45$, $t = 38.08$	3.68	0.0551	0.058	NA	5	NA

NA: Not available

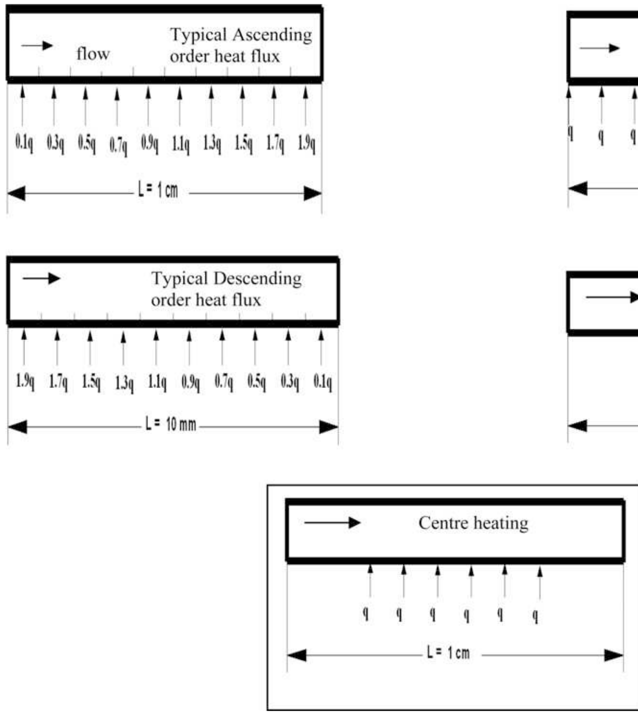

Fig. 8. Nonuniform base heat flux distribution in single and double stack heat sinks.

For the present analysis, a 10 mm × 10 mm copper heat sink is considered for analysis. The different kinds of nonuniformities in the base heat flux considered for the analysis are shown in Fig. 8.

A. Single Stack Heat Sinks

For single stack heat sinks, two cases of heat flux nonuniformities, upstream half heating and downstream half heating, are studied. The results are compared to the uniform heating case. Fig. 9 shows the base temperature distribution for nonuniform heating (and uniform heating as well) of a parallel flow heat sink.

Note that the base temperatures for nonuniform heating are higher than for uniform heating due to the concentration of heat in the upstream or downstream part. For the case of downstream half heating, it can be observed that there is some increase in the base temperature even in the upstream part. This is mainly because of axial heat conduction. Also, the base temperature is highest for downstream heating due to preheating of the coolant due to axial conduction of heat into the upstream half. The corresponding thermal resistances for the above cases are given in Table II. Note that R is at a maximum for downstream heating followed by upstream heating and is at a minimum for uniform heating throughout the base.

Fig. 10 gives the base temperature distribution for nonuniform heating of the counterflow heat sink. For the case of the counterflow heat sink, the temperature distribution pattern and the peak temperatures are almost the same for the upstream (initial half) and downstream (latter half) heating since the coolant flows in opposite directions through adjacent channels. Obviously, the higher temperatures lie in the initial section of the channel for upstream half heating while, for downstream

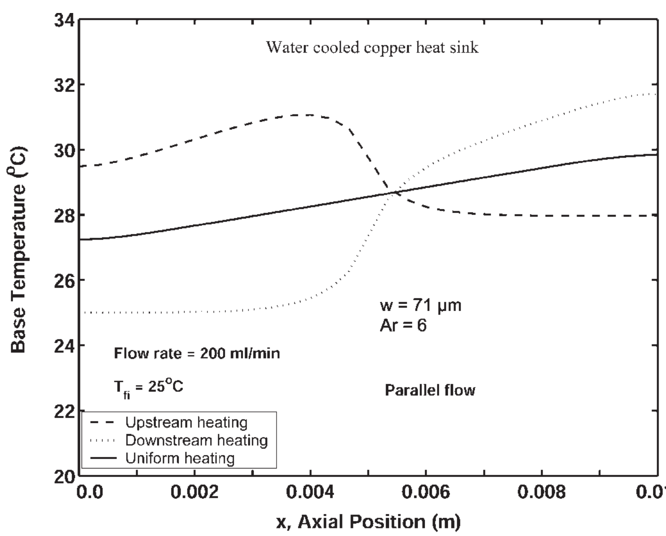

Fig. 9. Microchannel base temperature distributions in the streamwise direction for a single stack parallel flow heat sink.

Table II
Thermal Resistances for Nonuniform Heating of Single Stack Parallel Flow Heat Sink

	R (°C/W)
Upstream half heating	0.161
Downstream half heating	0.179
Uniform heating throughout the base	0.128

Flow rate = 200 mL/min

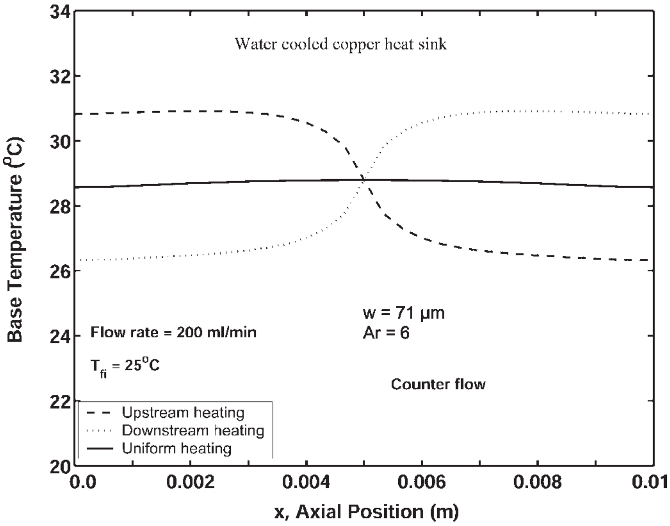

Fig. 10. Microchannel base temperature distributions in the streamwise direction for a single stack counterflow heat sink.

half heating, the higher temperatures lie in the latter half of the channel.

The corresponding thermal resistances for half heating cases and the uniform heating case are given in Table III. It can be noted that the thermal resistance is lowest for the case of uniform heating and that the thermal resistances are the same for both upstream half heating and downstream half heating. Also, a comparison of Tables II and III shows that the counterflow heat sink yields lower thermal resistance than the parallel flow heat sink for both the uniform and half heating cases.

Table III
Thermal Resistances for Nonuniform Heating of Single Stack Counterflow Heat Sink

	R (°C/W)
Upstream half heating	0.156
Downstream half heating	0.156
Uniform heating throughout the base	0.10

Flow rate = 200 mL/min

B. Multistack Heat Sinks

A 10 mm × 10 mm water cooled double stack copper heat sink with a channel aspect ratio of 3 is used for the analysis.

C. Base Heat Distribution in Ascending and Descending Order with Respect to the Flow Direction in the Bottom Channel

Fig. 11 shows the microchannel base temperature variation of the 10 mm × 10 mm double stack, water cooled parallel flow heat sink for ascending and descending order heat flux distributions. The base temperature distributions for uniform heating are added in the figures for comparison. It can be observed from Fig. 11 that for a parallel flow heat sink the heat flux distribution in ascending order yields the highest peak base temperature due to progressive heating of the channel and the coolant, and greater heat concentrations near the channel exit. Note that the descending order heat flux distribution yields the minimum peak base temperature (lower than the ascending order heat flux distribution case and the uniform heating case) and the temperature distribution is more uniform. Note from Fig. 11 that in the case of the descending order heat flux distribution, the base temperature is not maximum at the channel entry but increases gradually to reach a maximum somewhere in between the channel length and again decreases toward the channel exit. This is mainly because the coolant temperature is at a minimum at the channel entry and hence the convective heat transfer driving potential is at a maximum

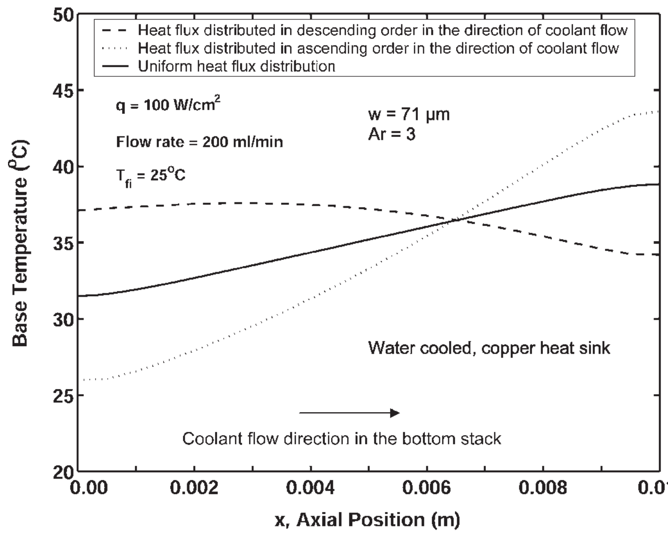

Fig. 11. Microchannel base temperature distribution of a parallel flow, double stack heat sink with nonuniform base heating.

at the channel entry, resulting in efficient heat removal. Thereafter, the channel temperature increases slowly in spite of the decrease in base heat flux (heat flux distribution being in descending order) mainly because the coolant gets heated up and the convective heat transfer driving potential ($T_w - T_f$) decreases. The base temperature starts decreasing only once the base heat flux becomes small enough to override the effects of decreasing ($T_w - T_f$). The uniform temperature distribution yields a peak base temperature lower than the ascending order heat flux distribution but higher than the case of descending order heat flux distribution.

Fig. 12 shows the microchannel base temperature variation for ascending and descending order heat flux distributions in an identical double stack counterflow heat sink. The base heat distributions for the case of uniform heating of the counterflow heat sink are also added in the above figures for comparison. For counterflow heat sinks, both ascending order and descending order heat flux distributions (with respect to the flow direction in the bottom channel) yield almost identical base temperature distribution patterns but in opposite directions. It can be observed that in the case of the counterflow heat sinks, the uniform heating case yields a more uniform base temperature distribution with the lowest peak temperature compared with the nonuniform heating cases.

The corresponding thermal resistances for nonuniform heating of the parallel flow and counterflow double stack heat sinks are given in Table IV. It can be observed from Table IV that the double stack parallel flow heat sink yields lower thermal resistance than the double stack counterflow heat sink for descending order heat flux distribution, while the double stack counterflow heat sink yields lower thermal resistance than the double stack parallel flow heat sink for the ascending order heat flux distribution and the uniform heating cases.

D. Upstream Half Heating, Downstream Half Heating, and Center Half Heating

Fig. 13 shows the microchannel base temperature variation of a 10 mm × 10 mm water cooled, double stack parallel flow, copper heat sink for the upstream half, downstream half, and center half heating cases.

For the parallel flow arrangement, the downstream half heating results in higher peak temperatures and also yields poorer temperature uniformity compared with the cases of upstream heating and center half heating. This is mainly because of preheating of the coolant in the upstream part (due to axial conduction of heat into the upstream half) as a result of which, the downstream half experiences higher coolant temperatures. Although heat is axially conducted even in the case of upstream half heating, the result is insignificant as there is no heat source in the downstream half. The upstream half and center half heating cases give almost the same peak temperature, but it can be observed that the upstream half heating yields a desirable more uniform base temperature.

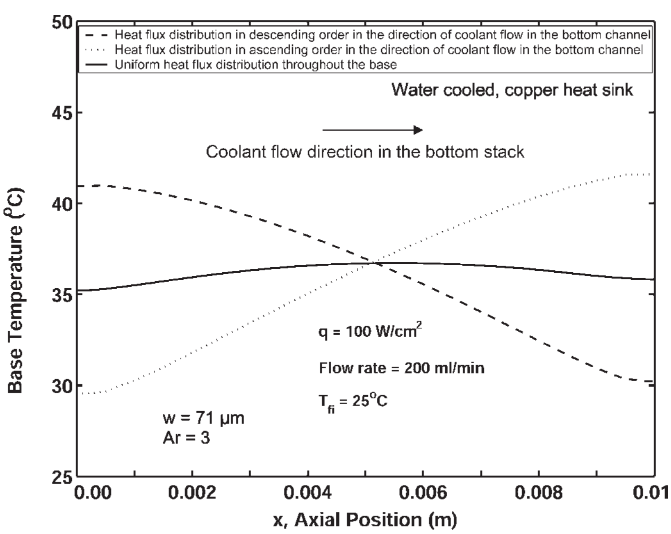

Fig. 12. Microchannel base temperature distribution of counterflow, double stack heat sink with nonuniform base heating.

Fig. 14 shows similar base temperature distributions for a double stack counterflow heat sink. In the case of the counterflow arrangement, the effect of axial heat conduction can be clearly observed for both upstream half and downstream heating. It is observed that the temperature distribution pattern for the upstream half heating and downstream half heating in

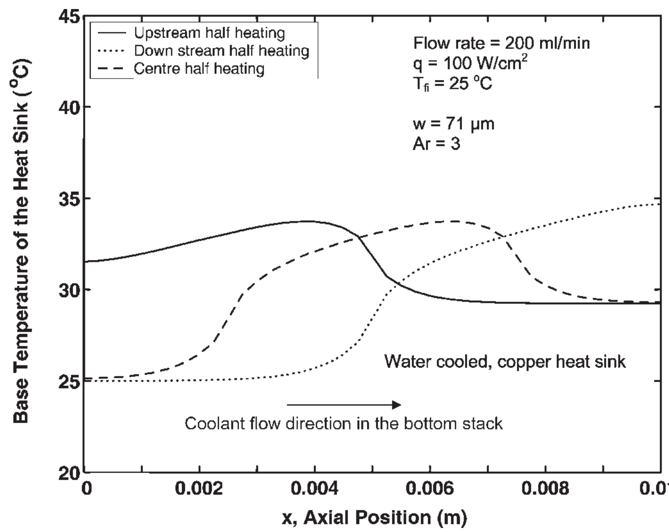

Fig. 13. Base temperature distribution for center half heating, upstream half heating, and downstream half heating of a double stack, parallel flow heat sink.

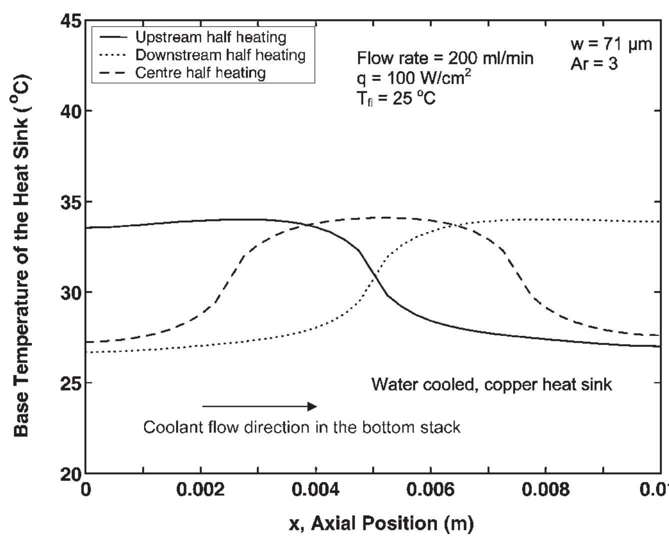

Fig. 14. Base temperature distribution for center half heating, upstream half heating, and downstream half heating of double stack, counterflow heat sink.

Table IV
Comparative Thermal Resistances of the Double Stack Parallel Flow and Counterflow Water Cooled Heat Sinks

	Double stack parallel flow heat sink			Double stack counter flow heat sink		
	Ascending order heat flux distribution	Descending order heat flux distribution	Uniform heating	Ascending order heat flux distribution	Descending order heat flux distribution	Uniform heating
R (°C/W)	0.186	0.126	0.138	0.1658	0.1595	0.117

Flow rate = 200 mL/min

Table V
Thermal Resistances of 10 mm × 10 mm Water Cooled Double Stack, Parallel Flow and Counterflow, Copper Heat Sinks for Different Partial Heating Cases

	Double stack parallel flow heat sink				Double stack counter flow heat sink			
	Upstream half heating	Downstream half heating	Center half heating	Uniform heating throughout the base	Upstream half heating	Downstream half heating	Center half heating	Uniform heating throughout the base
R (°C/W)	0.174	0.193	0.174	0.138	0.18	0.18	0.1812	0.117

Flow rate = 200 mL/min

the double stack counterflow heat sink are the same, but in the opposite directions. It is observed that the center half heating yields a slightly higher peak base temperature. The peak base temperatures for the upstream half heating and downstream half heating cases are almost the same.

Table V gives comparative thermal resistances for the double stack parallel flow and counterflow heat sinks. The thermal resistances for the uniform heating case are also added in the table for comparison. The following observations can be made from Table V.

1. For the double stack parallel flow heat sink, upstream half heating yields lower thermal resistances than downstream half heating. The thermal resistances for upstream half heating and center half heating are almost the same for the double stack parallel flow heat sink.
2. For the double stack counterflow heat sink, both upstream half heating and downstream half heating yield almost the same thermal resistance. However, center half heating yields higher thermal resistances than both upstream half heating and downstream half heating.
3. For both parallel flow and counterflow heat sinks, the case of uniform heating throughout the base yields lower thermal resistances than any of the partial heating cases. Also, for uniform heating it is observed that the counterflow heat sink yields lower thermal resistance than the parallel flow heat sinks.
4. For the case of upstream half heating, the parallel flow double stack heat sink yields lower thermal resistance than the counterflow heat sink. The parallel flow heat sink performs even better for the case of center half heating. However, the counterflow double stack heat sink performs better (yields lower thermal resistances) than the parallel flow double stack heat sink for the downstream half heating case and the uniform heating case.

Conclusions

The present work provides a simple and accurate method to analyze microchannel heat sinks. For single stack parallel flow heat sinks, it is observed that the thermal resistance R is at a maximum for downstream heating followed by upstream heating and is at a minimum for uniform heating throughout the base. For counterflow heat sinks, the thermal resistance is lowest for the case of uniform heating and the thermal resistances are almost same for both the upstream half heating case and the downstream half heating case. Also, the counterflow heat sink yields lower thermal resistance than the parallel flow heat sink for both the uniform heating case and the half heating case.

For the parallel flow double stack heat sink, the descending order heat flux distribution yields the minimum peak base temperature and the temperature distribution is more uniform. In the case of the counterflow heat sinks, uniform base heating yields a lower peak temperature compared with the nonuniform heating cases.

For the case of upstream half heating, the parallel flow double stack heat sink yields lower thermal resistance than the counterflow heat sink. The parallel flow heat sink performs even better for the case of center half heating. However, the counterflow double stack heat sink performs better (yields lower thermal resistances) than the parallel flow double stack heat sink for the downstream half heating case and the uniform heating case.

References

[1] D.B. Tuckerman and R.F. Pease, "High performance heat sinking for VLSI," IEEE Electron Device Letters, Vol. EDL-2, No. 4, pp. 126-129, 1981.

[2] R.J. Philips, "Advances in thermal modeling of electronic components," in A. Bar-Cohen and A.D. Kraus (Eds.), "*Microchannel Heat Sinks*," ASME, New York, 1990, pp. 109-184.

[3] S.J. Kim and D. Kim, "Forced convection in microstructures for electronic equipment cooling," ASME Journal of Heat Transfer, Vol. 21, pp. 639-645, 1999.

[4] A.G. Fedorov and R. Viskanta, "Three-dimensional conjugate heat transfer in the microchannel heat sink for electronic packaging," International Journal of Heat and Mass Transfer, R., Vol. 43, pp. 399-415, 2000.

[5] D.P. Kulkarni and D.K. Das, "Analytical and numerical studies on microscale heat sinks for electronic applications," Applied Thermal Engineering, Vol. 25, pp. 2432-2449, 2005.

[6] P. Hegde, "Microchannel heat sinks for cooling high heat flux electronic devices—Analysis with single and two phase flows," *Ph.D. Thesis*, University of Science, Malaysia, 2006.

[7] P. Hegde and K.N. Seetharamu, "Thermal analysis of micro-channel heat exchangers with two-phase flow using FEM," International Journal of Numerical Methods for Heat & Fluid Flow, Vol. 15, No. 1, pp. 43-60, 2005.

[8] P. Hegde, M.Z. Abdullah, K.N. Seetharamu, and P.A. Narayana, "Counter and parallel two-phase flow microchannel heat sinks for electronics cooling," International Journal of Heat Exchangers Vol. 7, No. 1, <http://edwardspub.com/journals/IJHEX/VII/57.pdf>, 2006.

[9] P. Naphon and O. Khonseur, "Study on the convective heat transfer and pressure drop in the micro-channel heat sink," International Communications in Heat and Mass Transfer, Vol. 36, pp. 39-44, 2009.

[10] S.H. Chong, K.T. Ooi, and T.N. Wong, "Optimization of single and double layer counter flow microchannel heat sinks," Applied Thermal Engineering, Vol. 22, pp. 1569-1585, 2002.

[11] X. Wei and Y.K. Joshi, "Stacked microchannel heat sinks for liquid cooling of microelectronic components," ASME Journal of Electronic Packaging, Vol. 126, pp. 60-65, 2004.

[12] R.K. Shah and A.L. London, "Laminar flow forced convection in ducts: A sourcebook for compact heat exchanger analytical data," in: T.F. Irvine and J.P. Hartnett (Eds.), "*Advances in Heat Transfer*," Academic Press, New York, 1978.

[13] R.W. Lewis, P. Nithiarasu, and K.N. Seetharamu, "*Fundamentals of the Finite Element Method for Heat and Fluid Flow*," John Wiley and Sons, New York, 2004.